

# Basolateral Uptake of Nucleosides by Sertoli Cells Is Mediated Primarily by Equilibrative Nucleoside Transporter 1<sup>§</sup>

David M. Klein, Kristen K. Evans, Rhiannon N. Hardwick, William H. Dantzler, Stephen H. Wright, and Nathan J. Cherrington

Department of Pharmacology and Toxicology (D.M.K., R.N.H., N.J.C.) and Department of Physiology (K.K.E., W.H.D., S.H.W.), University of Arizona, Tucson, Arizona

Received January 14, 2013; accepted May 1, 2013

## ABSTRACT

The blood-testis barrier (BTB) prevents the entry of many xenobiotic compounds into seminiferous tubules thereby protecting developing germ cells. Understanding drug transport across the BTB may improve drug delivery into the testis. Members of one class of drug, nucleoside reverse transcriptase inhibitors (NRTIs), do not penetrate the BTB, presumably through interaction with physiologic nucleoside transporters. By investigating the mechanism of nucleoside transport, it may be possible to design other drugs to bypass the BTB in a similar manner. We present a novel *ex vivo* technique to study transport at the BTB that employs isolated, intact seminiferous tubules. Using this system, we found that over 80% of total uptake by seminiferous tubules of the model nucleoside uridine could be inhibited by 100 nM nitrobenzylmercaptapurine riboside (NBMPR, 6-S-

[(4-nitrophenyl)methyl]-6-thioinosine), a concentration that selectively inhibits equilibrative nucleoside transporter 1 (ENT1) activity. In primary cultured rat Sertoli cells, 100 nM NBMPR inhibited all transepithelial transport and basolateral uptake of uridine. Immunohistochemical staining showed ENT1 to be located on the basolateral membrane of human and rat Sertoli cells, whereas ENT2 was located on the apical membrane of Sertoli cells. Transepithelial transport of uridine by rat Sertoli cells was partially inhibited by the NRTIs zidovudine, didanosine, and tenofovir disoproxil fumarate, consistent with an interaction between these drugs and ENT transporters. These data indicate that ENT1 is the primary route for basolateral nucleoside uptake into Sertoli cells and a possible mechanism for nucleosides and nucleoside-based drugs to undergo transepithelial transport.

## Introduction

The anatomic portion of the blood-testis barrier (BTB) is composed of tight junctions formed between the Sertoli cells that line the seminiferous tubules inside the testis (Mital, et al., 2011; Pelletier, 2011; Li et al., 2012). This barrier prevents many exogenous agents from gaining entry into the lumen of the seminiferous tubules and contacting germ cells. It is also the responsibility of the Sertoli cells to provide nutrients such as nucleosides that allow for spermatogenesis (Kato et al., 2009; Mruk and Cheng, 2011). Although this barrier is beneficial for sperm cell development, it can be an obstacle for drugs that are required to bypass the BTB to achieve full therapeutic effect. Examples of such drugs include many antiretroviral medications used to treat infection of human immunodeficiency virus (HIV). By limiting the entry of many antiretrovirals into the male genital tract

(MGT), the BTB may be contributing to the testes' serving as a sanctuary site for HIV (Byrn and Kiessling, 1998; Anderson et al., 2000; Olson et al., 2002; Dahl et al., 2010). Because the tight junctions of the BTB prevent paracellular diffusion of hydrophilic drugs, transcellular transport through the Sertoli cells is required for antiretrovirals to bypass the BTB.

One class of HIV antiretrovirals, nucleoside reverse transcriptase inhibitors (NRTIs), may be able to bypass the BTB (Pereira et al., 2002; Augustine et al., 2005; Else et al., 2011). Clinical data have shown seminal plasma concentrations of zidovudine (AZT, 3'-azido-3'-deoxythymidine) and didanosine (ddI, 2',3'-dideoxyinosine) are up to 10-fold higher than blood plasma (Lowe et al., 2007; Dumond et al., 2008). Understanding the transepithelial transport pathway NRTIs use to bypass the BTB could potentially be useful in designing other drugs to cross into the lumen of seminiferous tubules.

Because NRTIs are nucleoside analogs, these medications may use the same nucleoside transport pathway(s) used by endogenous nucleosides such as uridine. Kato et al. (2005), representing the field's understanding of the physiologic pathway for nucleosides crossing the BTB, found that uridine uptake into primary Sertoli cells is dominated by two sodium

This work was supported by the National Institutes of Health National Institute of Allergy and Infectious Diseases [Grants AI083927, ES006694, and HD062489].

dx.doi.org/10.1124/jpet.113.203265.

<sup>§</sup> This article has supplemental material available at [jpet.aspetjournals.org](http://jpet.aspetjournals.org).

**ABBREVIATIONS:** AZT, zidovudine, 3'-azido-3'-deoxythymidine; ddI, didanosine, 2',3'-dideoxyinosine; BTB, blood-testis barrier; CNT, concentrative nucleoside transporter; DMEM/F-12, Dulbecco's modified Eagle's medium/Ham's F-12; DMSO, dimethylsulfoxide; ENT, equilibrative nucleoside transporter; IHC, immunohistochemistry; HIV, human immunodeficiency virus; MGT, male genital tract; NBMPR, nitrobenzylmercaptapurine riboside, 6-S-[(4-nitrophenyl)methyl]-6-thioinosine; NRTI, nucleoside reverse transcriptase inhibitor; RLU, relative light units; WB, Waymouth buffer.

independent components that possess characteristics similar to equilibrative transporter 1 (ENT1) and equilibrative transporter 2 (ENT2). ENT proteins are bidirectional transporters that facilitate nucleosides transport according to concentration gradient (Ward et al., 2000; Baldwin et al., 2004).

The function of ENT1 and ENT2 is commonly differentiated based on their relative sensitivity to nitrobenzylmercaptapurine riboside (NBMPR, 6-S-[(4-nitrophenyl)methyl]-6-thioinosine): ENT1 is very sensitive to NBMPR inhibition ( $K_i = 0.1$  to  $68.5$  nM), and ENT2 is unaffected by NBMPR at concentrations up to  $1$   $\mu$ M but is blocked by  $100$   $\mu$ M NBMPR (Griffiths et al., 1997; Takano et al., 2010; Yao et al., 2011; Abd-Elfattah et al., 2012; Nishimura et al., 2012). ENT1 and ENT2 have been shown to transport AZT and are speculated to transport other NRTI drugs as well (Ward et al., 2000; Pastor-Anglada et al., 2005). It also has been shown that basolateral entry of nucleosides into Sertoli cells is ENT dependent, although it has not been clear whether ENT1, ENT2, or both are involved (Kato et al., 2005).

A minor sodium-dependent component also found to contribute to uridine uptake is believed to be a concentrative nucleoside transporter (CNT). CNT proteins are unidirectional uptake transporters that typically localize to the apical membrane of epithelial cells and usually play a role in nucleoside salvaging (Lu et al., 2004; Kato et al., 2005; Errasti-Murugarren et al., 2012). NBMPR does not interact with CNT transporters, which allows it to be a tool for distinguishing between ENT- and CNT-mediated transport (Ritzel et al., 2001; Kong et al., 2004; Fernandez-Calotti et al., 2011; Nishimura et al., 2012).

Despite the work done on nucleoside transport in Sertoli cells, there are still many gaps in our current understanding. For example, previous studies have not localized nucleoside transporters to the apical or basolateral membrane, nor have they demonstrated whether ENT1, ENT2, or both are responsible for basolateral nucleoside uptake. Our study addresses these questions. We determined the kinetic and selectivity characteristics of transport of the representative nucleoside uridine in intact seminiferous tubules *ex vivo*. Primary cultured Sertoli cells isolated from rat testes were analyzed for their ability to transport uridine. We performed immunohistochemical (IHC) analysis on both rat and human tissue to localize ENT1 and ENT2. These results support the conclusions that 1) rat ENT1 (rENT1) and human ENT1 (hENT1) are located on the basolateral membrane of Sertoli cells, 2) ENT1 is primarily responsible for basolateral nucleoside uptake into Sertoli cells, and 3) rENT2 and hENT2 are localized to the apical membrane.

## Materials and Methods

The Quantigene HV Signal Amplification Kit and the Quantigene Discovery Kit were purchased from Genospectra (Fremont, CA). Oligonucleotide probe sets for ENT1, ENT2, CNT1, and CNT2 were developed as published previously (Augustine et al., 2005). The CNT3 sequence was obtained from the National Institutes of Health GenBank, and the target sequences were analyzed by ProbeDesigner software version 1.0 (Genospectra). The probes were designed with a melting temperature of approximately  $63^\circ\text{C}$ , enabling hybridization conditions to be held constant at  $53^\circ\text{C}$  for each oligonucleotide probe set (Supplemental Table 1). Every probe developed through the ProbeDesigner software was searched with the Basic Local Alignment Search Tool (BLAST) against the nucleotide database to ensure

minimal or no cross-reactivity with other known rat sequences or expressed sequence tags. RNazol B reagent was purchased from Tel-Test (Friendswood, TX). Nonradiolabeled uridine, Dulbecco's modified Eagle's medium/Ham's F-12 medium (DMEM/F-12) medium, tenofovir disoproxil fumarate, AZT, and ddI were purchased from Sigma-Aldrich (St. Louis, MO). NBMPR was purchased from Santa Cruz Biotechnology (Santa Cruz, CA). Stock solutions of NBMPR were made with dimethylsulfoxide (DMSO). MACH4 IHC staining kit was acquired from Biocare Medical (St. Louis, MO). [ $^3\text{H}$ ]Uridine (specific activity:  $30.1$  Ci/mMol) was purchased from American Radio-labeled Chemicals (St. Louis, MO). ENT1 (SLC29A1) and the ENT2 (SLC29A2) rabbit antibodies were purchased from Lifespan Biosciences (Seattle, WA), and their quality was determined by the manufacturer. BD Matrigel Matrix and the transwell inserts used for primary Sertoli cell cultures were purchased from BD Biosciences (San Jose, CA). All other reagents were purchased from a standard scientific supplier at the highest available purity.

**Branched DNA Assay.** Specific oligonucleotide probes for ENT1, ENT2, CNT1, CNT2, and CNT3 were diluted in lysis buffer supplied by the Quantigene HV Signal Amplification Kit. The substrate solution, lysis buffer, capture hybridization buffer, amplifier, and label probe buffer used in the analysis were all obtained from the Quantigene Discovery Kit. The assay was performed in 96-well format with the RNA isolated from seminiferous tubules added to the capture hybridization buffer and  $50$   $\mu$ l of the diluted probe set. The total RNA was then allowed to hybridize to the probe set overnight at  $53^\circ\text{C}$ . Hybridization steps were performed per the manufacturer's protocol the next day. Luminescence of the samples was measured with a Quantiplex 320 bDNA luminometer interfaced with Quantiplex Data Management Software, version 5.02 (Bayer, Walpole, MA). The total RNA was isolated from rat seminiferous tubules or rat kidney tissue by use of RNazol B reagent per the manufacturer's protocol. The integrity of the RNA was confirmed by ethidium bromide staining after agarose gel electrophoresis. The background for each transporter was determined using negative control wells that had all reagents except for the RNA. The background was then subtracted to demonstrate the expression above the background levels.

**Ex Vivo Transport Experiments with Intact Seminiferous Tubules.** All protocols for obtaining animal tissue samples were approved by the University of Arizona institutional review board or the institutional animal care and use committee. Seminiferous tubules were dissected from rat or mouse testes in chilled Ringer's solution containing (mM):  $103$  NaCl,  $25$  NaHCO<sub>3</sub>,  $19$  sodium gluconate,  $1$  sodium acetate,  $1.2$  NaH<sub>2</sub>PO<sub>4</sub>,  $5$  KCl,  $1$  CaCl<sub>2</sub>,  $1$  MgCl<sub>2</sub>, and  $5.5$  glucose at pH  $7.4$ . Images of the tubules were then taken for measurements of length needed to normalize the data. Uptake baths containing [ $^3\text{H}$ ]uridine in Ringer's solution, alone or with varied concentrations of unlabeled uridine or NBMPR, were covered with oil to prevent evaporation and brought to a temperature of  $35^\circ\text{C}$ . Individual tubules were transferred by a glass needle into the appropriate bath for a given period of time, and then transferred to wells containing  $1$  N NaOH for extraction of accumulated radioactivity, which was subsequently measured by an LS 6000 scintillation counter manufactured by Beckman (Ramsey, MN). At least three individual tubules were analyzed for each condition in all experiments. For studies using NBMPR, the concentration of DMSO was equal in all uptake baths and never exceeded  $1\%$ .

**Sertoli Isolation.** Sertoli cell isolation was performed using the protocol of Mruk and Cheng (2011). Briefly, the tunica was separated from the seminiferous tubules, then the tubules were cut into  $1$  mm pieces, incubated in  $50/50$  mixture of DMEM/F-12 medium, and resuspended in media with  $0.002\%$  DNase and  $0.1\%$  trypsin to release the interstitial cells. After washing and resuspension, the medium was replaced with a DMEM/F-12 medium with  $1$  M glycine and  $2$  mM EDTA to lyse the interstitial cells. The cells were resuspended in DMEM/F-12 medium with  $0.1\%$  collagenase and  $0.005\%$  DNase to remove the myoid layer. After washing, the cells were given a fresh DMEM/F-12 medium with  $0.1\%$  hyaluronidase and  $0.005\%$  DNase to

break down the extracellular matrix. Cells were then plated at a density of  $0.5 \times 10^6$  cells/cm<sup>2</sup> onto transwell inserts previously coated with a thin layer of Matrigel (diluted 1:7 with media) as per the manufacturer's instructions (BD Biosciences). The cell medium was supplemented with epidermal growth factor and human transferrin. After 36 to 48 hours at 37°C, the cells were treated with a 20 mM tris buffer (pH 7.4) for 2.5 minutes to lyse germ cells and then given fresh DMEM/F-12 medium supplemented with epidermal growth factor and human transferrin. The cells were then incubated at 37°C and cultured for an additional 4 days (6 days total from isolation). The medium was changed as needed, typically every 1 to 2 days.

**Primary Sertoli Cell Transport Experiments.** Once the cells were confluent (day 6), the medium was replaced with Waymouth buffer containing (WB; mM): 135 NaCl, 13 HEPES, 2.5 CaCl<sub>2</sub>, 1.2 MgCl<sub>2</sub>•6H<sub>2</sub>O, 0.8 MgSO<sub>4</sub>•7H<sub>2</sub>O, 5 KCl, 28 D-glucose at pH 7.4. To measure the basolateral-to-apical transepithelial uridine flux, the cells were incubated at room temperature for 10 minutes before the buffer in the basolateral compartment was replaced with WB containing 1 μCi/ml of [<sup>3</sup>H]uridine (approximately 30 nM) plus additional test agent (NBMPR, unlabeled uridine, or NRTI drug) as required. At selected time intervals, WB from the apical compartment was removed and assessed for radioactivity via liquid scintillation spectroscopy.

To determine the rate of uridine transport across the basolateral membrane, WB in the apical compartment was replaced with white paraffin oil. At 15 minutes, the cells were lysed with 0.5 N NaOH, 1% SDS solution for 20 minutes. The NaOH was neutralized using 1 N HCl. The radioactivity in the extract was measured by liquid scintillation spectroscopy. Each point represents an average of data collected in triplicate. For studies using NBMPR, the concentration for DMSO did not exceed 1%.

**Sample Collection.** Animal samples were collected from euthanized rats either 21 days old (immature) or at least 2 months old (mature). The samples were fixed in 10% neutral buffered formalin overnight. A small incision was made in the tunica the next day, and the samples remained in 10% neutral buffered formalin for another night. The next day, formalin was replaced with 70% ethanol until the samples were embedded in paraffin. Paraffin-embedded human samples were purchased from the National Disease Research Interchange (NDR) or were provided from the University of Arizona Medical Center pathology department. Patients had testis removed as part of therapy for prostate cancer. Human testis tissue was evaluated by a local pathologist and determined to be normal. Sectioning of all paraffin-embedded tissue was accomplished using a microtome with sections sliced 5 microns thick with one section per slide. Protocols for obtaining samples were approved by the University of Arizona institutional review board or institutional animal care and use committee.

**Immunohistochemistry.** IHC staining was performed on formalin-fixed, paraffin-embedded samples. Slides were deparaffinized with xylene and rehydrated with ethanol. The samples were then heated in an antigen retrieval buffer: citrate (pH 6.0) for ENT1, or tris-EGTA (pH 9.0) for ENT2. Endogenous peroxidase activity was blocked by a 0.3% hydrogen peroxide/methanol solution. Staining for ENT1 and ENT2 was performed with the MACH4 kit according to the manufacturer's instructions (Biocare Medical). All slides were imaged with a Leica DM4000B microscope and a DFC450 camera (Leica Microsystems, Buffalo Grove, IL).

**Statistics.** Data are presented as the mean ± S.E., with the sample size representing separate experiments (each typically performed in triplicate). All tests of statistical significance of observed differences were done by one-way analysis of variance using a Tukey post hoc multiple comparison test, with  $P < 0.05$  considered statistically significant.

## Results

**Basolateral Uptake of [<sup>3</sup>H]Uridine by Rodent Seminiferous Tubules.** To analyze the role of ENT transporters

in nucleoside transport across the BTB, we measured the ability of intact isolated single rodent seminiferous tubules to accumulate [<sup>3</sup>H]uridine, thereby providing a measure of basolateral uptake. Figure 1 shows a time course for [<sup>3</sup>H]uridine basolateral uptake in seminiferous tubules for the rat (Fig. 1A) and mouse (Fig. 1B). The concentrations of [<sup>3</sup>H]uridine in the bath were 0.41 μM for the rat, and 1.88 μM for the mouse. Transport for both rat and mouse tubules was nearly linear for the first 5 minutes. Accumulation of [<sup>3</sup>H]uridine into rat tubules was reduced by 54 to 83% over the first 20 minutes in the presence of 5 mM unlabeled uridine, suggesting that uridine uptake involved a saturable process.

The basolateral uptake of [<sup>3</sup>H]uridine in both rat and mouse seminiferous tubules was inhibited by increasing concentrations of unlabeled uridine in a manner adequately described using the Michaelis-Menten equation for the competitive interaction of labeled and unlabeled substrate introduced by Malo and Berteloot (1991). In five separate experiments, the  $K_t$  values for uridine transport were  $314 \pm 63$  μM and  $90 \pm 24$  μM,

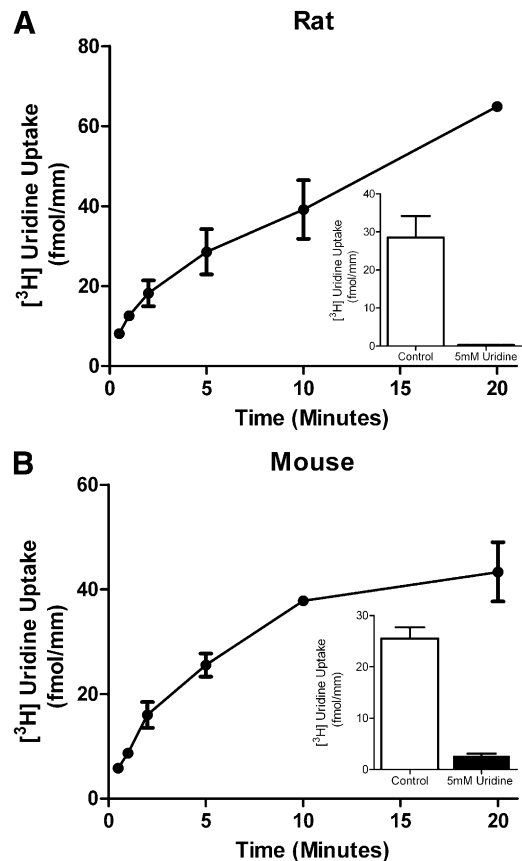


**Fig. 1.** Time course of basolateral transport of [<sup>3</sup>H]uridine by rodent seminiferous tubules. Composite graphs depicting [<sup>3</sup>H]uridine transport by rat (A) or mouse (B) intact seminiferous tubules through the basolateral surface over time. The mean concentration of [<sup>3</sup>H]uridine in the baths were 0.41 and 1.88 μM for rats and mice, respectively. [<sup>3</sup>H]Uridine transport in the presence of 5 mM unlabeled uridine was analyzed to determine the saturable portion of uridine transport in rat seminiferous tubules. The insets demonstrate the saturable uptake of rat or mouse seminiferous tubules at 5 minutes with and without the presence of 5 mM uridine. Each point represents the mean (± S.E.) of four experiments for rats and two experiments for mice (± half the range), each with a different animal. At least three tubules per time point were analyzed in each experiment.

and the  $J_{\max}$  values were  $2.5 \pm 0.6$  pmol/(min-mm) and  $0.55 \pm 0.2$  pmol/(min-mm) for rat and mouse seminiferous tubules, respectively. Figure 2 shows the kinetic profiles for uridine uptake into these tubules, corrected for the nonsaturable component of total uridine uptake.

Because uridine is commonly used as a substrate for ENT-mediated transport, it was anticipated that this process would be inhibited by NBMPR, a potent inhibitor of ENT1 and a weak inhibitor of ENT2. The interaction between NBMPR and uridine transport is shown in Fig. 3. The  $IC_{50}$  of NBMPR on [ $^3$ H]uridine was calculated by using the following equation (Groves et al., 1994):

$$J = \frac{J_{\text{app}}[\text{Uridine}^*]}{IC_{50} + [\text{NBMPR}]_0} + D[\text{Uridine}^*]$$

where  $J$  is the rate of [ $^3$ H]uridine uptake;  $J_{\text{app}}$  is the product of the maximum rate of [ $^3$ H]uridine uptake ( $J_{\max}$ ) and the ratio of the  $K_i$  of NBMPR and  $K_t$  for uridine transport; and  $IC_{50}$  is the concentration of [NBMPR] $_0$  that reduced mediated (i.e., blockable) [ $^3$ H]uridine transport by 50%. The concentration of NBMPR was carried out to 500 nM, but maximal inhibition

was achieved by 100 nM for both rats and mice. NBMPR inhibited this transport with an  $IC_{50}$  for the mediated (i.e., blockable) fraction of [ $^3$ H]uridine uptake of  $23.6 \pm 3.1$  nM for rat tubules (Fig. 3A) and  $12.9 \pm 0.7$  nM for mouse tubules (Fig. 3B). These  $IC_{50}$  values are similar to the range of  $IC_{50}$  values (0.1 to 68.5 nM) reported for ENT1 by others (Griffiths et al., 1997; Takano et al., 2010).

The 400 nM concentration of NBMPR did not appear to block uridine uptake into seminiferous tubules to the same extent as 5 mM unlabeled uridine (compare Fig. 2 with Fig. 3, A and B). To compare the inhibition of NBMPR to that of unlabeled uridine, seminiferous tubules were categorized into four groups based on supplements in the media: control (no supplements), 5 mM uridine, 400 nM NBMPR, or 100  $\mu$ M NBMPR (Fig. 3C). The control group was statistically significantly different from the other groups, and there was also a statistically significant difference between the 5 mM uridine and the 400 nM NBMPR groups. No statistically significant difference was found between the other pairings. These data suggest that ENT2 plays no significant role in basolateral uridine transport, but that a small fraction (18.8%) of that accumulation may involve a pathway other than ENT1.

**Basolateral Uptake of [ $^3$ H]Uridine by Primary Rat Sertoli Cells.** To characterize the contribution of Sertoli cells to [ $^3$ H]uridine uptake by seminiferous tubules, primary Sertoli cells were isolated from rat testes, and [ $^3$ H]uridine basolateral uptake was characterized on Matrigel-coated transwell plates. Figure 4 shows a time course of basolateral-to-apical (transepithelial transport) of [ $^3$ H]uridine across primary cultured Sertoli cells. By 15 minutes, radiolabel appeared in the apical compartment. This signal was completely blocked at all time points by the addition of 5 mM uridine, 100 nM NBMPR, or 100  $\mu$ M NBMPR.

Because ENT transporters are bidirectional, primary Sertoli cells were exposed to NBMPR and [ $^3$ H]uridine in the basolateral compartment followed by light paraffin oil application on the apical side (which prevents apical efflux of the hydrophilic uridine) to determine whether inhibition of the transepithelial transport of [ $^3$ H]uridine was mediated by basolateral uptake or cellular efflux across the apical membrane. Figure 5 shows the 15-minute accumulation of [ $^3$ H]uridine into Sertoli cells across the basolateral membrane. That accumulation was reduced by 95% in the presence of 100 nM NBMPR, indicating that the inhibition of transepithelial transport seen in Fig. 4 was due to the blocking of [ $^3$ H]uridine basolateral uptake into Sertoli cells.

**mRNA Expression of Nucleoside Transporters in Fresh Seminiferous Tubules.** In the light of evidence of CNT expression in primary cultured Sertoli cells (Kato et al., 2005), we determined the mRNA expression of nucleoside transporters in freshly isolated rat seminiferous tubules, freshly isolated Sertoli cells, and primary Sertoli cells cultured for 6 days. Figure 6 shows the branched DNA analysis of freshly isolated seminiferous tubules (6A) and primary Sertoli cells (6B). Expression of nucleoside transporters in seminiferous tubules was normalized to rat kidney tissue (which is known to express ENT1, ENT2, CNT1, CNT2, and CNT3), expressed in relative light units (RLU) (Rodriguez-Mulero et al., 2005; Ishida et al., 2013). ENT1 expression was approximately 2.53-fold higher in seminiferous tubules than in kidney tissue. ENT2 expression was also highly expressed, with

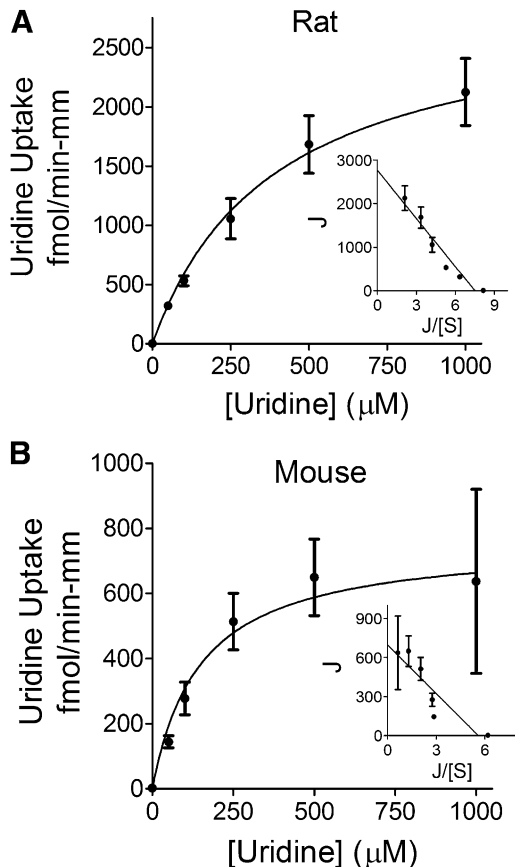


**Fig. 2.** Ex vivo kinetic analysis of basolateral transport of [ $^3$ H]uridine by rodent seminiferous tubules. Composite graphs demonstrating basolateral [ $^3$ H]uridine transport by rat (A) or mouse (B) intact seminiferous tubules in the presence of increasing concentrations of unlabeled uridine. The mean concentrations of [ $^3$ H]uridine in the baths were 0.45 and 0.37  $\mu$ M for rats and mice, respectively. The  $K_t$  values were calculated to be 314 and 90  $\mu$ M for rat and mouse seminiferous tubules, respectively. Each point represents an average ( $\pm$  S.E.) of at least five different experiments, each with a different animal. Insets demonstrate Eadie-Hofstee transformation of the data. At least three separate tubules for each unlabeled uridine concentration were analyzed in each experiment.

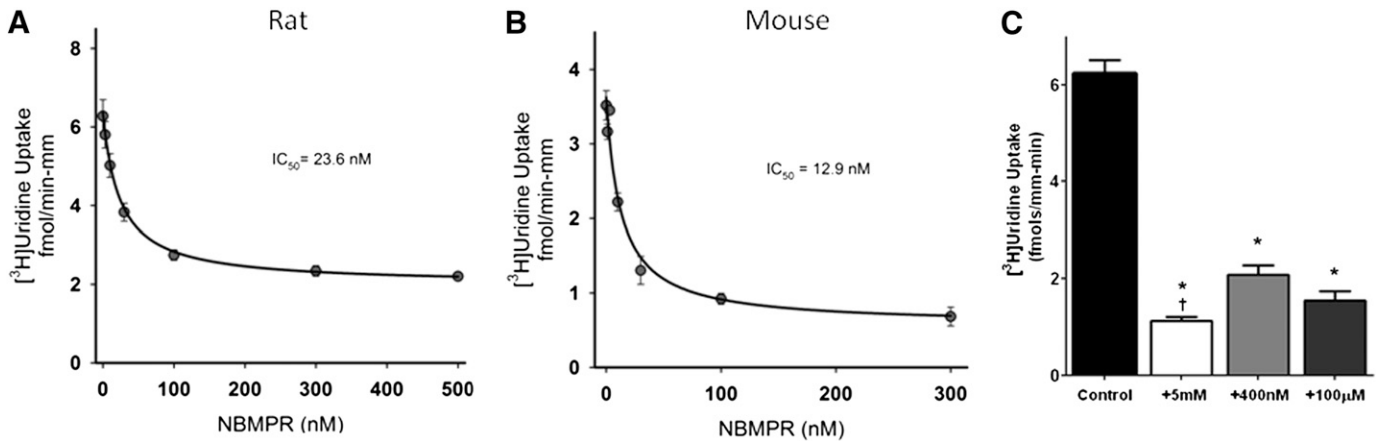


**Fig. 3.** Ex vivo analysis of the effects of NBMPR on basolateral transport of [ $^3\text{H}$ ]uridine by rodent seminiferous tubules. Composite graphs depicting [ $^3\text{H}$ ]uridine transport by rat (A) or mouse (B) intact seminiferous tubules in the presence of increasing concentrations of NBMPR. The mean concentrations of [ $^3\text{H}$ ]uridine in the baths were 0.43 and 1.11  $\mu\text{M}$  for rats and mice, respectively. The  $\text{IC}_{50}$  values were calculated to be 23.6 and 12.9 nM for rat and mouse seminiferous tubules, respectively. Each point represents an average ( $\pm$  S.E.) of at least five experiments, each with a different animal. At least three separate tubules for each NBMPR concentration were analyzed in each experiment. The bar graph (C) represents ex vivo basolateral uptake of [ $^3\text{H}$ ]uridine in intact rat seminiferous tubules. The mean concentration of [ $^3\text{H}$ ]uridine in the baths was 45  $\mu\text{M}$ . Control represents [ $^3\text{H}$ ]uridine uptake in the absence of NBMPR or unlabeled uridine. [ $^3\text{H}$ ]uridine transport in the presence of 5 mM unlabeled uridine was analyzed to determine the saturable portion of uridine transport. The concentrations of NBMPR are enough to block just ENT1 activity (400 nM) or both ENT1 and ENT2 (100  $\mu\text{M}$ ). The height of each bar is 6.22 (control), 1.12 (5 mM uridine), 2.08 (400 nM NBMPR), and 1.55 (100  $\mu\text{M}$  NBMPR)  $\text{fmols mm}^{-1} \text{min}^{-1}$ . \*Statistical significance ( $P < 0.05$ ) compared with control. †Statistical significance ( $P < 0.05$ ) compared with 400 nM NBMPR.

RLU readings of 0.94 compared with the kidney. Expression of CNT1, CNT2, and CNT3 was much lower than that of ENT1 or ENT2 (0.05-, 0.09-, and 0.05-fold, respectively).

In primary Sertoli cells, RLU values were normalized to glyceraldehyde-3-phosphate dehydrogenase. ENT1 was found to be highly expressed ( $0.44 \pm 0.14$  and  $0.35 \pm 0.07$  RLU for days 0 and 6, respectively) as was ENT2 ( $0.75 \pm 0.33$  and  $0.45 \pm 0.12$  for days 0 and 6, respectively). Small amounts of CNT1 were detected ( $0.04 \pm 0.01$  and  $0.04 \pm 0.02$  for days 0 and 6, respectively) but CNT2 and CNT3 expression was below background. No statistically significant difference in transporter expression was observed between the freshly isolated cells (day 0) and the cells cultured for 6 days (day 6).

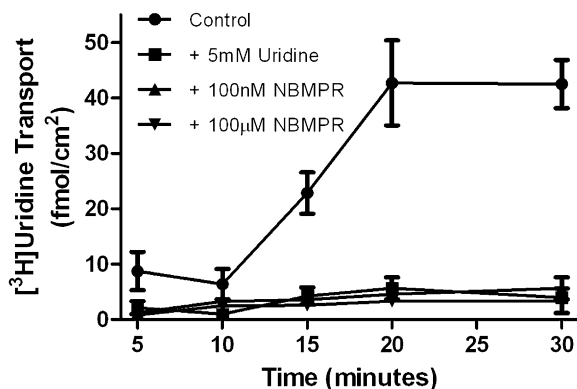


**Fig. 4.** In vitro analysis of role of rENT1 and rENT2 in [ $^3\text{H}$ ]uridine transepithelial transport by primary cultured Sertoli cells. Confluent monolayers of primary cultured rat Sertoli cells were exposed to 40 nM [ $^3\text{H}$ ]uridine in the basolateral compartment. Apical media was counted to determine the transepithelial transport. Cells were exposed to concentrations of NBMPR sufficient to inhibit ENT1 (100 nM), ENT2 and ENT1 (100  $\mu\text{M}$ ), or unlabeled uridine (5 mM). Control cells were not given NBMPR or unlabeled uridine. The lines describing the data were fit by eye. Each point represents an average ( $\pm$  S.E.) of triplicate wells of Sertoli cells derived from a mixture of three rats.

**Immunohistochemical Staining of Rat and Human Testes.** IHC staining for ENT1 and ENT2 was performed on rat testes to determine the subcellular distribution of these transporters. rENT1 and rENT2 were localized in Sertoli cells using IHC staining on both immature (Fig. 7, A and C) and

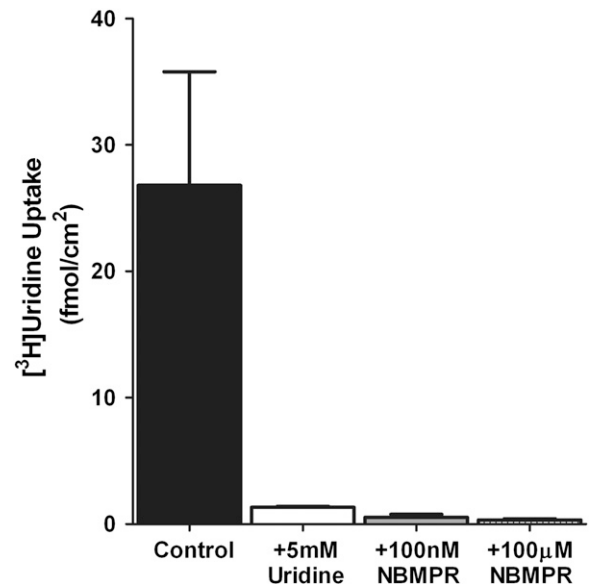


**Fig. 5.** Effects of NBMPR on the basolateral uptake of [ $^3\text{H}$ ]uridine in primary cultured rat Sertoli cells. Confluent monolayers of primary cultured rat Sertoli cells were provided with 40 nM [ $^3\text{H}$ ]uridine in the basolateral compartment. After 15 minutes, the cells were lysed, and the lysates were counted to determine cellular accumulation of [ $^3\text{H}$ ]uridine. The cells were exposed to concentrations of NBMPR sufficient to inhibit ENT1 uptake (100 nM), ENT2 and ENT1 (100  $\mu\text{M}$ ), or unlabeled uridine (5 mM). Control cells were not given NBMPR or unlabeled uridine. Each point represents an average ( $\pm$  half the range) of duplicate wells of Sertoli cells derived from a mixture of three rats. The height of each bar is 26.81 (control), 1.33 (5 mM uridine), 0.53 (400 nM NBMPR), and 0.34 (100  $\mu\text{M}$  NBMPR)  $\text{fmol mm}^{-1} \text{min}^{-1}$ .

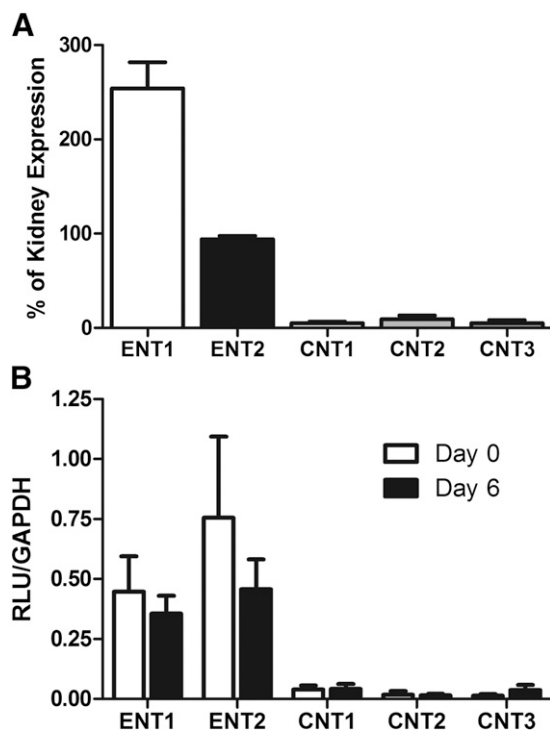


**Fig. 6.** Branched DNA analysis of nucleoside transporter expression in seminiferous tubules relative to kidney. RNA extracted from freshly isolated seminiferous tubules or kidney tissue (A) from four rats was analyzed for expression of ENT1, ENT2, CNT1, CNT2, and CNT3. To account for variations among probe sets, the expression of each transporter was compared with kidney as a positive control. Graph depicts above background expression relative to positive control. Expression: ENT1 253.9%, ENT2 94.0%, CNT1 5.2%, CNT2 9.3%, and CNT3 5.2% relative to kidney expression. Each point represents the mean ( $\pm$  S.E.) of six wells. RNA extracted from freshly isolated Sertoli cells or 6-day cultured Sertoli cells (B) from four rats was also analyzed for expression of ENT1, ENT2, CNT1, CNT2, and CNT3. All RLU values were normalized to glyceraldehyde-3-phosphate dehydrogenase (GAPDH) expression. RLU values freshly isolated primary Sertoli cells (day 0): ENT1 0.44, ENT2 0.75, CNT1 0.04, CNT2 0.02, and CNT3 0.01. RLU values for cultured primary Sertoli cells (day 6): ENT1 0.35, ENT2 0.46, CNT1 0.04, CNT2 0.01, and CNT3 0.03. Each point represents the mean ( $\pm$  S.E.) of three wells.

mature (Fig. 7, B and D) rats. In both mature and immature testes, rENT1 was located on the basolateral membrane of Sertoli cells (Fig. 7, A and B). In contrast, slides stained for rENT2 expressed positive staining on the apical membrane but not on the basolateral membrane (Fig. 7, C and D).

IHC staining was also performed on adult human testes to determine whether hENT1 and hENT2 share the same localization as their rat counterparts (Fig. 8). Consistent with the expression profiles observed in the rat testis, IHC staining revealed the presence of hENT1 on the basolateral membrane (Fig. 8A) and hENT2 on the apical membrane (Fig. 8B) of the Sertoli cells.

**NRTI Inhibition of [ $^3$ H]Uridine Transport by Primary Cultured Rat Sertoli Cells.** To determine whether the transporters used by uridine could also interact with NRTIs, the transepithelial transport of uridine by primary Sertoli cells was measured in the presence of the NRTIs AZT (5 mM), ddI (5 mM), and tenofovir disoproxil fumarate (1 mM). Each of these NRTIs significantly inhibited uridine transepithelial transport (Fig. 9). The ability of these drugs to block basolateral uridine transport supports the contention that

these NRTIs interact with the same transporter(s) used by uridine and may also act as substrates.

## Discussion

We present a novel ex vivo technique for determining BTB transport using freshly isolated seminiferous tubules. Using both this novel ex vivo and traditional in vitro systems that employed 6-day cultured Sertoli cells, we demonstrated that, based on pharmacologic inhibition by NBMPR, basolateral uptake of nucleosides by Sertoli cells is dominated by ENT1. We also demonstrate that ENT2 does not play a significant role in basolateral uridine uptake into Sertoli cells. NBMPR inhibited 66% of total uridine uptake in rat seminiferous tubules at concentrations that pharmacologically inhibit ENT1 but do not affect ENT2 (100 nM) (Ward et al., 2000; Abd-Elfattah et al., 2012; Nishimura et al., 2012) (Fig. 3, A and B). Of the saturable component (i.e., the portion of transport blocked by 5 mM unlabeled uridine), 400 nM NBMPR inhibited 81% of uridine transport; increasing the NBMPR concentration to 100  $\mu$ M (sufficient to block ENT2) did not result in a significant decrease in uridine uptake (Fig. 3C). This strongly implicates ENT1 as the primary transporter in nucleoside uptake into seminiferous tubules.

The results with intact tubules were confirmed and extended by the observations in the primary cultured rat Sertoli cells. In these Sertoli cells, 100 nM NBMPR blocked the entire saturable portion of transepithelial uridine transport (Fig. 4), supporting the contention that transepithelial transport of uridine past the BTB depends on functional ENT1. Importantly, this inhibition was also observed in the basolateral uptake of uridine (Fig. 5), strongly supporting the conclusion that ENT1 mediates the basolateral entry for the transepithelial transport of uridine across Sertoli cells.

We also discovered that ENT2 is located on the apical membrane and not on the basolateral membrane. This is based on three observations. First, IHC data located ENT2 to the apical membrane but not to the basolateral membrane (Fig. 8). Second, inhibition of ENT1 (via 100 nM NBMPR) virtually stops all transepithelial transport of uridine across the basolateral membrane of Sertoli cells (Fig. 5). Third, increasing NBMPR concentration from 100 nM to 100  $\mu$ M had little further effect on inhibition of uridine uptake (Figs. 4 and 5). These data demonstrate that ENT2 must play little to no role in basolateral uptake of uridine into seminiferous tubules.

Interestingly, in seminiferous tubules, there was a small portion (approximately 19%) of [ $^3$ H]uridine transport that was blocked by unlabeled uridine but not by high concentrations of NBMPR. Because NBMPR can prevent transport of uridine in Sertoli cells, this unexplained accumulation may not reflect activity of Sertoli cells. Perhaps it is due to some effect of the myoid layer, which is removed during Sertoli cell isolation. However, because such a large proportion of uptake into the tubules is blocked by 100 nM NBMPR (which has no effect on CNT-mediated transport), ENT1 seems to be the primary transporter responsible for nucleoside uptake into seminiferous tubules. This is in agreement with expression of ENT1 but not ENT2 on the basolateral membrane of Sertoli cells. The identical localizations of ENT1 and ENT2 in both rat and human tissues suggest that data gathered from rat Sertoli cells and seminiferous tubules may be applicable to



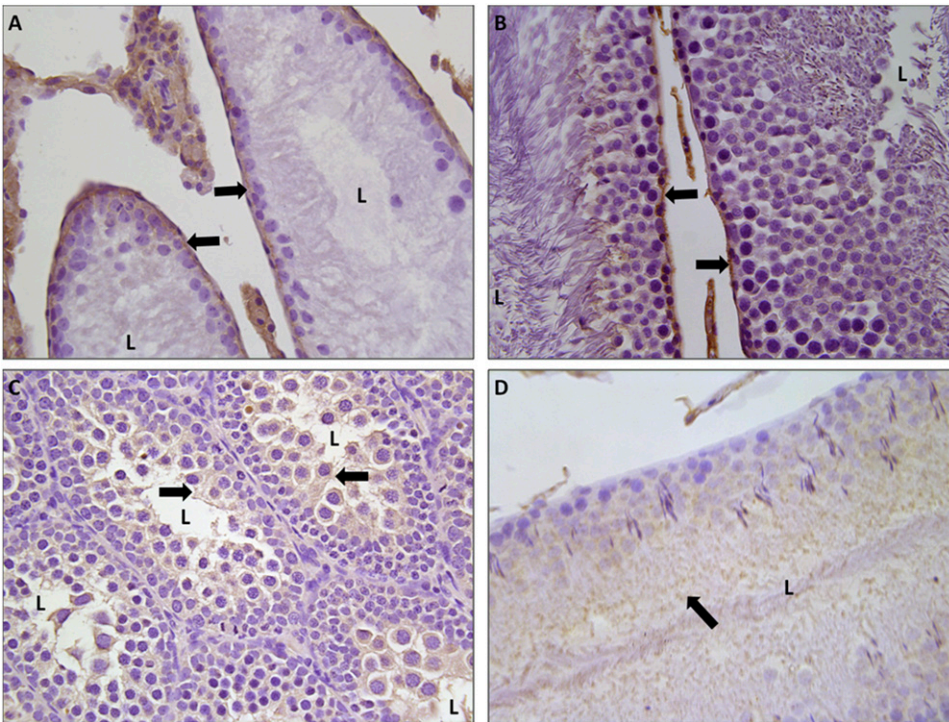


**Fig. 7.** Localization of rENT1 and rENT2 in the testis. Immunohistochemical staining for ENT1 (A and B) or ENT2 (C and D) in formalin-fixed paraffin-embedded immature (A and C) or mature (B and D) rat testes is shown at 40 $\times$  magnification. Arrows indicate positive (brown) staining for proteins. L, lumen of seminiferous tubules.

humans. Unfortunately, fresh human seminiferous tubules were unavailable, so uptake studies with human seminiferous tubules could not be performed.

We also demonstrated through branched DNA analysis that ENTs are the primary nucleoside transporters expressed in fresh seminiferous tubules, fresh Sertoli cells, and 6-day cultured primary Sertoli cells; all had low to undetectable expression of CNTs (Fig. 6). Furthermore, the complete inhibition of basolateral uridine uptake produced by 100 nM NBMPR suggests that CNTs do not exert an appreciable impact on basolateral transport of uridine in Sertoli cells (Figs. 4 and 5). This would indicate that any CNTs expressed by Sertoli cells, which bDNA analysis suggests to be very modest, would be localized to the apical membrane.

Whereas the function of ENT1 on the basolateral membrane is evident, the role of ENT2 on the apical membrane is less clear. A common physiologic function of ENT transporters is to transport nucleosides from the blood into the cell, and this is how we believe ENT1 functions in Sertoli cells (Kato et al., 2005; Molina-Arcas et al., 2008). As ENT1 transports

nucleosides into the cell, the intracellular concentration of these molecules could rise to approach that in the blood. Because ENT transporters move nucleosides according to their concentration gradient, ENT2 on the apical membrane would transport nucleosides from inside the cell into the lumen of the seminiferous tubule where they can be used by developing germ cells. These dividing germ cells could act as a “nucleoside sink,” keeping the luminal nucleoside concentration low enough to drive unidirectional transport. Figure 10 provides an illustration of how this hypothesized process could be functioning to transport nucleosides into the lumen. To the extent that CNTs are expressed in the apical membrane of Sertoli cells, their activity would be expected to reabsorb some fraction of the nucleoside secreted by ENT2. Because we suspect that the CNTs impact on nucleoside transport into native Sertoli cells is likely to be minimal (see earlier discussion), we do not expect these transporters to have a substantial impact on nucleoside transport. Clearly, more studies involving ENT2 and CNTs on the apical membrane of Sertoli cells are required to verify this model.

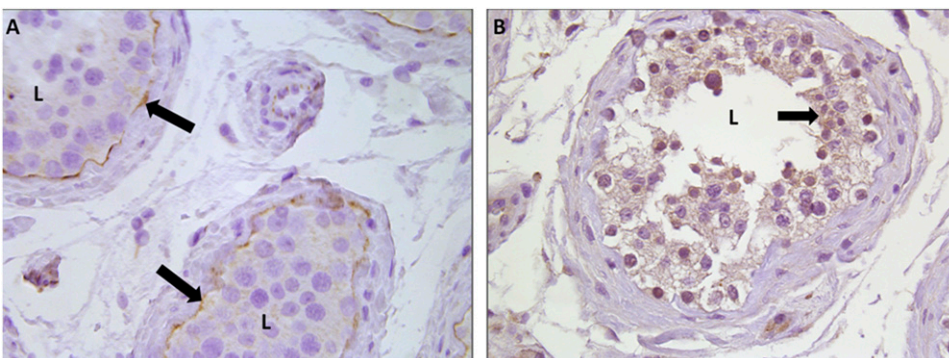


**Fig. 8.** Localization of hENT1 and hENT2 in the testis. Immunohistochemical staining for ENT1 (A) or ENT2 (B) in formalin-fixed paraffin-embedded adult human testes is shown at 40 $\times$  magnification. Arrows indicate positive (brown) staining for proteins. L, lumen of seminiferous tubules.

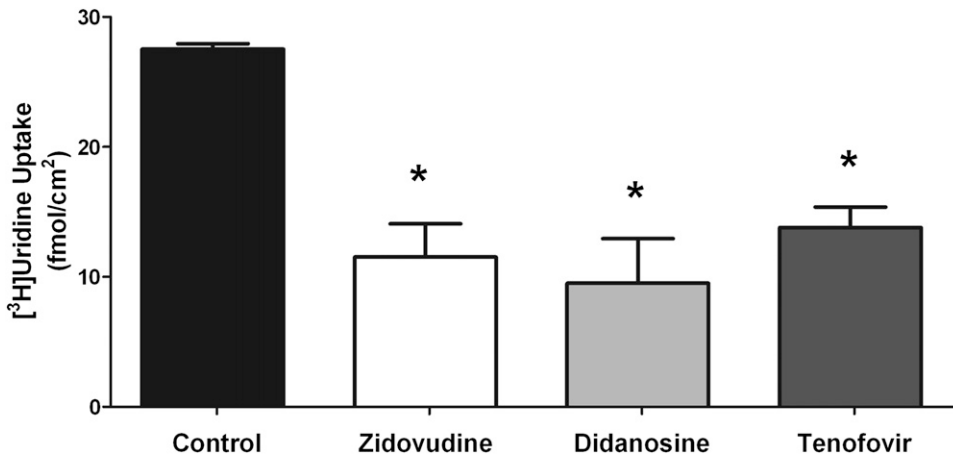


**Fig. 9.** Inhibition of [<sup>3</sup>H]uridine transport by NRTI in primary cultured rat Sertoli cells. Confluent monolayers of primary cultured rat Sertoli cells were exposed to media in the basolateral compartment containing 40 nM [<sup>3</sup>H]uridine and either AZT (5 mM), ddI (5 mM), or tenofovir disoproxil fumarate (TDF; 1 mM). Control wells were not exposed to any NRTI drugs. Media from the apical compartments were counted to assess trans-epithelial transport of [<sup>3</sup>H]uridine after 15 minutes. Each bar represents an average (± S.E.) of triplicate wells of Sertoli cells derived from a mixture of three rats. The height of each bar is 27.52 (control), 11.52 (AZT), 9.51 (ddI), and 13.79 (TDF). \*Statistically significant (*P* < 0.05) compared with control.

Using this model, if the NRTI concentration inside the seminiferous tubules rose above that of the blood, then ENT2 and ENT1 would remove drug from the tubules and transport it back into the blood. This would suggest that the concentration of NRTI drugs would never rise above that of the blood in the seminiferous tubule. This is puzzling because clinical data have indicated that NRTI drugs are up to 10-fold more concentrated in seminal plasma than in blood plasma (Dumond et al., 2008). One possible explanation could be that NRTI drugs reach concentrations similar to blood levels in the seminiferous tubules but are then concentrated farther down

the MGT. Fluid from the seminiferous tubule flows into the epididymis where up to 99% of the water can be reabsorbed (Lu et al., 2008; Cornwall, 2009). Assuming the drug is not also reabsorbed, this would increase the concentration of drug approximately 100-fold. During ejaculation, the drug from the epididymis would mix with secretions from accessory sex organs (primarily secretions originating from the seminal vesicles and prostate), resulting in dilution of the drug (Van Praag et al., 2001; Cao et al., 2008; Caballero et al., 2012). As testicular fluid has been estimated to contribute up to 10% of the total volume for semen, this would dilute the drug to roughly 10-fold above blood concentration (Van Praag et al., 2001). This illustrates a possible mechanism for drugs crossing the BTB and then becoming concentrated in the MGT, resulting in a higher concentration of drug in the seminal plasma than in blood plasma.

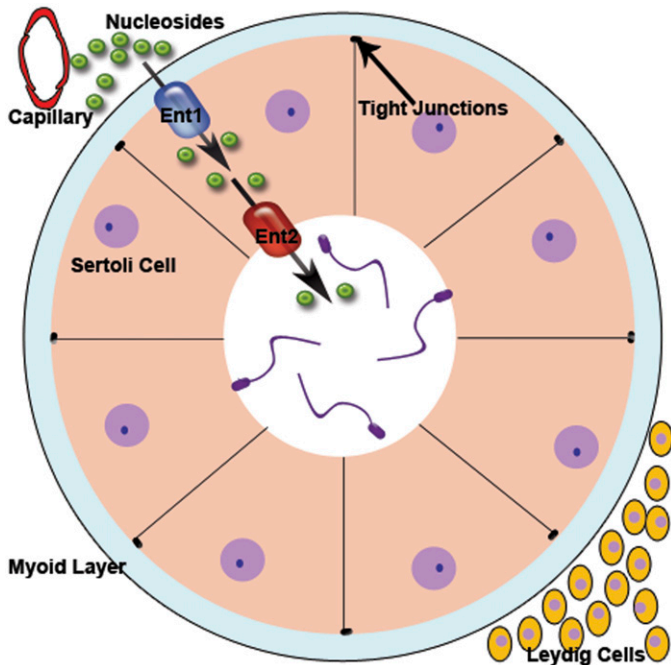


**Fig. 10.** Model of ENT-mediated transport of nucleosides across the BTB. The illustration of the seminiferous tubule and surrounding cells depicts how nucleosides could be transported into the lumen via ENT transporters. ENT1 is the primary transporter responsible for uptake of nucleosides into the Sertoli cells owing to the higher concentration of nucleosides in the blood. ENT2 is proposed to play a role in efflux of nucleosides into the lumen of the seminiferous tubules because of the higher concentration of intracellular nucleosides (mediated by ENT1) compared with the lumen of the seminiferous tubule.

The assumption that a drug is not reabsorbed in the epididymis requires further investigation. Studies investigating epididymal drug transport are limited, but one study revealed that ENT1, ENT2, and CNT2 are present in the epididymis (Leung et al., 2001). Without knowing the localization of these transporters, it is difficult to speculate on their potential impact on drug transport. If, for example, CNT2 is the only nucleoside transporter on the apical membrane, then pyrimidine-based analogs such as zidovudine and lamivudine would not be reabsorbed because CNT2 transports purine-based analogs (Van Aubel et al., 2000; Gray et al., 2004).

This ENT dominant system is a possible mechanism for NRTI transport at the BTB. We have shown that ENTs are localized in Sertoli cells in a manner that would support transepithelial transport, that ENT1 is necessary for basolateral nucleoside transport, and that some NRTIs can inhibit the transepithelial transport of uridine, which indicates that they interact with the same transporters (Fig. 9). This is in agreement with other sources that have demonstrated that ENT transporters can transport NRTIs (Ward et al., 2000). Taken together, these data indicate the possibility of a novel ENT-mediated pathway for the penetration of nucleosides and NRTIs past the BTB.

**Acknowledgments**

The authors thank the NIH-funded National Disease Research Interchange and Rob Klein (University of Arizona Medical Center) for providing paraffin-embedded human samples.



## Authorship Contributions

Participated in research design: Klein, Evans, Hardwick, Dantzler, Wright, Cherrington.

Conducted experiments: Klein, Evans.

Contributed new reagents or analytic tools: Evans.

Performed data analysis: Klein, Evans, Hardwick, Dantzler, Wright, Cherrington.

Wrote or contributed to the writing of the manuscript: Klein, Dantzler, Wright, Cherrington.

## References

- Abd-Elfattah AS, Ding M, Jessen ME, and Wechsler AS (2012) On-pump inhibition of es-ENT1 nucleoside transporter and adenosine deaminase during aortic cross-clamping entraps intracellular adenosine and protects against reperfusion injury: role of adenosine A1 receptor. *J Thorac Cardiovasc Surg* **144**:243–249.
- Anderson PL, Noormohamed SE, Henry K, Brundage RC, Balfour HH, Jr, and Fletcher CV (2000) Semen and serum pharmacokinetics of zidovudine and zidovudine-glucuronide in men with HIV-1 infection. *Pharmacotherapy* **20**:917–922.
- Augustine LM, Markelewicz RJ, Jr, Boekelheide K, and Cherrington NJ (2005) Xenobiotic and endobiotic transporter mRNA expression in the blood-testis barrier. *Drug Metab Dispos* **33**:182–189.
- Baldwin SA, Beal PR, Yao SY, King AE, Cass CE, and Young JD (2004) The equilibrative nucleoside transporter family, SLC29. *Pflugers Arch* **447**:735–743.
- Byrn RA and Kiessling AA (1998) Analysis of human immunodeficiency virus in semen: indications of a genetically distinct virus reservoir. *J Reprod Immunol* **41**:161–176.
- Caballero I, Parrilla I, Almiñana C, del Olmo D, Roca J, Martínez EA, and Vázquez JM (2012) Seminal plasma proteins as modulators of the sperm function and their application in sperm biotechnologies. *Reprod Domest Anim* **47** (Suppl 3):12–21.
- Cao YJ, Caffo B, Choi L, Radebaugh CL, Fuchs EJ, and Hendrix CW (2008) Non-invasive quantitation of drug concentration in prostate and seminal vesicles: improvement and validation with desipramine and aspirin. *J Clin Pharmacol* **48**:176–183.
- Cornwall GA (2009) New insights into epididymal biology and function. *Hum Reprod Update* **15**:213–227.
- Dahl V, Josefsson L, and Palmer S (2010) HIV reservoirs, latency, and reactivation: prospects for eradication. *Antiviral Res* **85**:286–294.
- Dumond JB, Reddy YS, Troiani L, Rodriguez JF, Bridges AS, Fiscus SA, Yuen GJ, Cohen MS, and Kashuba AD (2008) Differential extracellular and intracellular concentrations of zidovudine and lamivudine in semen and plasma of HIV-1-infected men. *J Acquir Immune Defic Syndr* **48**:156–162.
- Else LJ, Taylor S, Back DJ, and Khoo SH (2011) Pharmacokinetics of antiretroviral drugs in anatomical sanctuary sites: the male and female genital tract. *Antivir Ther* **16**:1149–1167.
- Errasti-Murugarren E, Fernández-Calotti P, Veyhl-Wichmann M, Diepold M, Pinilla-Macua I, Pérez-Torras S, Kipp H, Koepsell H, and Pastor-Anglada M (2012) Role of the transporter regulator protein (RS1) in the modulation of concentrative nucleoside transporters (CNTs) in epithelia. *Mol Pharmacol* **82**:59–67.
- Fernández-Calotti PX, Colomer D, and Pastor-Anglada M (2011) Translocation of nucleoside analogs across the plasma membrane in hematologic malignancies. *Nucleosides Nucleotides Nucleic Acids* **30**:1324–1340.
- Gray JH, Owen RP, and Giacomini KM (2004) The concentrative nucleoside transporter family, SLC28. *Pflugers Arch* **447**:728–734.
- Griffiths M, Yao SY, Abidi F, Phillips SE, Cass CE, Young JD, and Baldwin SA (1997) Molecular cloning and characterization of a nitrobenzylthioinosine-insensitive (*ei*) equilibrative nucleoside transporter from human placenta. *Biochem J* **328**:739–743.
- Groves CE, Evans KK, Dantzler WH, and Wright SH (1994) Peritubular organic cation transport in isolated rabbit proximal tubules. *Am J Physiol* **266**:F450–458.
- Ishida K, Fukao M, Watanabe H, Taguchi M, Miyawaki T, Matsukura H, Uemura O, Zhang Z, Unadkat JD, and Hashimoto Y (2013) Effect of salt intake on bio-availability of mizoribine in healthy Japanese males. *Drug Metab Pharmacokinet* **28**:75–80.
- Kato R, Maeda T, Akaike T, and Tamai I (2005) Nucleoside transport at the blood-testis barrier studied with primary-cultured sertoli cells. *J Pharmacol Exp Ther* **312**:601–608.
- Kato R, Maeda T, Akaike T, and Tamai I (2009) Characterization of nucleobase transport by mouse Sertoli cell line TM4. *Biol Pharm Bull* **32**:450–455.
- Kong W, Engel K, and Wang J (2004) Mammalian nucleoside transporters. *Curr Drug Metab* **5**:63–84.
- Leung GP, Ward JL, Wong PY, and Tse CM (2001) Characterization of nucleoside transport systems in cultured rat epididymal epithelium. *Am J Physiol Cell Physiol* **280**:C1076–C1082.
- Li N, Wang T, and Han D (2012) Structural, cellular and molecular aspects of immune privilege in the testis. *Front Immunol* **3**:152.
- Lu DY, Li Y, Bi ZW, Yu HM, and Li XJ (2008) Expression and immunohistochemical localization of aquaporin-1 in male reproductive organs of the mouse. *Anat Histol Embryol* **37**:1–8.
- Lu H, Chen C, and Klaassen C (2004) Tissue distribution of concentrative and equilibrative nucleoside transporters in male and female rats and mice. *Drug Metab Dispos* **32**:1455–1461.
- Malo C and Berteloot A (1991) Analysis of kinetic data in transport studies: new insights from kinetic studies of Na(+)-D-glucose cotransport in human intestinal brush-border membrane vesicles using a fast sampling, rapid filtration apparatus. *J Membr Biol* **122**:127–141.
- Mital P, Hinton BT, and Dufour JM (2011) The blood-testis and blood-epididymis barriers are more than just their tight junctions. *Biol Reprod* **84**:851–858.
- Molina-Arcas M, Trigueros-Motos L, Casado FJ, and Pastor-Anglada M (2008) Physiological and pharmacological roles of nucleoside transporter proteins. *Nucleosides Nucleotides Nucleic Acids* **27**:769–778.
- Mruk DD and Cheng CY (2011) An in vitro system to study Sertoli cell blood-testis barrier dynamics. *Methods Mol Biol* **763**:237–252.
- Nishimura T, Chishu T, Tomi M, Nakamura R, Sato K, Kose N, Sai Y, and Nakashima E (2012) Mechanism of nucleoside uptake in rat placenta and induction of placental CNT2 in experimental diabetes. *Drug Metab Pharmacokinet* **27**:439–446.
- Olson DP, Scadden DT, D'Aquila RT, and De Pasquale MP (2002) The protease inhibitor ritonavir inhibits the functional activity of the multidrug resistance related-protein 1 (MRP-1). *AIDS* **16**:1743–1747.
- Pastor-Anglada M, Cano-Soldado P, Molina-Arcas M, Lostao MP, Larráyoz I, Martínez-Picado J, and Casado FJ (2005) Cell entry and export of nucleoside analogues. *Virus Res* **107**:151–164.
- Pelletier RM (2011) The blood-testis barrier: the junctional permeability, the proteins and the lipids. *Prog Histochem Cytochem* **46**:49–127.
- Pereira AS, Smeaton LM, Gerber JG, Acosta EP, Snyder S, Fiscus SA, Tidwell RR, Gulick RM, Murphy RL, and Eron JJ, Jr (2002) The pharmacokinetics of amprenavir, zidovudine, and lamivudine in the genital tracts of men infected with human immunodeficiency virus type 1 (AIDS clinical trials group study 850). *J Infect Dis* **186**:198–204.
- Lowe SH, van Leeuwen E, Droste JA, van der Veen F, Reiss P, Lange JM, Burger DM, Repping S, and Prins JM (2007) Semen quality and drug concentrations in seminal plasma of patients using a didanosine or didanosine plus tenofovir containing antiretroviral regimen. *Ther Drug Monit* **29**:566–570.
- Ritzel MW, Ng AM, Yao SY, Graham K, Loewen SK, Smith KM, Ritzel RG, Mowles DA, Carpenter P, and Chen XZ, et al. (2001) Molecular identification and characterization of novel human and mouse concentrative Na<sup>+</sup>-nucleoside cotransporter proteins (hCNT3 and mCNT3) broadly selective for purine and pyrimidine nucleosides (system cib). *J Biol Chem* **276**:2914–2927.
- Rodríguez-Mulero S, Errasti-Murugarren E, Ballarín J, Felipe A, Doucet A, Casado FJ, and Pastor-Anglada M (2005) Expression of concentrative nucleoside transporters SLC28 (CNT1, CNT2, and CNT3) along the rat nephron: effect of diabetes. *Kidney Int* **68**:665–672.
- Takano M, Kimura E, Suzuki S, Nagai J, and Yumoto R (2010) Human erythrocyte nucleoside transporter ENT1 functions at ice-cold temperatures. *Drug Metab Pharmacokinet* **25**:351–360.
- Van Aubel RA, Masereeuw R, and Russel FG (2000) Molecular pharmacology of renal organic anion transporters. *Am J Physiol Renal Physiol* **279**:F216–F232.
- van Praag RM, Repping S, de Vries JW, Lange JM, Hoetelmans RM, and Prins JM (2001) Pharmacokinetic profiles of nevirapine and indinavir in various fractions of seminal plasma. *Antimicrob Agents Chemother* **45**:2902–2907.
- Ward JL, Sherali A, Mo ZP, and Tse CM (2000) Kinetic and pharmacological properties of cloned human equilibrative nucleoside transporters, ENT1 and ENT2, stably expressed in nucleoside transporter-deficient PK15 cells. Ent2 exhibits a low affinity for guanosine and cytidine but a high affinity for inosine. *J Biol Chem* **275**:8375–8381.
- Yao SY, Ng AM, Cass CE, Baldwin SA, and Young JD (2011) Nucleobase transport by human equilibrative nucleoside transporter 1 (hENT1). *J Biol Chem* **286**:32552–32562.

Address correspondence to: Nathan J. Cherrington, 1703 E. Mabel, P.O. Box 210207, Tucson, AZ 85721. E-mail: cherrington@pharmacy.arizona.edu